Arch. Metall. Mater. **70** (2025), 2, 1055-1065

DOI: https://doi.org/10.24425/amm.2025.153511

M. IBRAHIM[1,2], W.M.W. IBRAHIM[2,3*], M.M. AL BAKRI ABDULLAH[1,2], A. ROMISUHANI[2], P. POSTAWA[4], S. ISHAK[5], R. EDIATI[6]

OPTIMIZATION OF METAKAOLIN-BASED ALKALI ACTIVATED MATERIALS FOR EFFICIENT COPPER REMOVAL FROM WASTEWATER

This study investigates the potential of metakaolin-based alkali-activated materials (AAM) as efficient adsorbents for copper removal through adsorption. The optimization process involved comparing the synthesis of AAM using metakaolin as the precursor material under two conditions: one with adding foaming agents, specifically hydrogen peroxide with a surfactant, and the other without any foaming agent. Characterization techniques, including specific surface area (BET), X-ray diffraction (XRD), and scanning electron microscopy (SEM), were employed to analyze the structural and morphological changes of the synthesized AAM. Batch adsorption experiments were conducted to evaluate the copper removal efficiency of the optimized AAM by considering factors such as initial copper concentration and pH. The Langmuir and Freundlich isotherm models were employed to investigate the adsorption mechanism and equilibrium behavior, providing insights into the adsorption process. The results demonstrated that the optimal AAM exhibited superior copper adsorption performance, achieving a removal efficiency of over 90% and best fitted with Langmuir isotherm suggesting that copper ions perform as a single molecule layer for MK-based AAM adsorption. This study contributes to the development of sustainable and effective materials for water treatment, particularly for addressing copper contamination. Metakaolin-based AAM with 1.00 wt.% hydrogen peroxide indicated the availability of numerous active sites for binding with Cu^{2+} and showed promise as a high-effective, convenient, and eco-friendly adsorbent for copper removal, with potential applications in various industrial and environmental settings.

Keywords: Metakaolin based alkali activated materials; adsorbent; adsorption; copper removal; wastewater treatment

1. Introduction

The presence of heavy metals in industrial wastewater poses a significant risk to public health [1], necessitating the treatment of wastewater before it can be released into the environment. Currently, standard methods for treating industrial heavy metal wastewater include chemical coagulation [2], ion-exchange [3,4] membrane filtration [5,6], flotation [7,8] and adsorption [9-11]. Among these methods, adsorption is widely favored because of its removes various heavy metals, such as lead, mercury, copper, and nickel [12-15].

Adsorption has demonstrated excellent performance in the removal of different heavy metal contaminants. They can effectively capture and bind heavy metal ions to the surface of adsorbent material, preventing their release into the environment [16-18]. This versatility makes adsorption an attractive option for treating industrial wastewater that contains various heavy metals. Adsorption processes have been optimized to achieve high heavy metal removal efficiencies. Adsorbent materials possess specific surface properties that selectively attract and adsorb heavy metal ions from wastewater, effectively removing them [19]. This characteristic is significant when dealing with complex wastewater streams containing multiple heavy metal contaminants.

Various adsorbent materials, including activated carbon, zeolites, clay minerals, and biochar, can be employed for heavy metal adsorption [20,21]. These materials offer diverse surface chemistries, pore structures, and functional groups, which enhance their affinities for different heavy metal ions [22,23]. The choice of adsorbent can be tailored to the specific heavy

[1] UNIVERSITI MALAYSIA PERLIS (UNIMAP), FACULTY OF CHEMICAL ENGINEERING & TECHNOLOGY, 02600, ARAU, PERLIS, MALAYSIA
[2] UNIVERSITI MALAYSIA PERLIS (UNIMAP), CENTER OF EXCELLENCE GEOPOLYMER AND GREEN TECHNOLOGY (CEGEOGTECH), 01000, PERLIS, MALAYSIA
[3] UNIVERSITI MALAYSIA PERLIS (UNIMAP), FACULTY OF MECHANICAL ENGINEERING & TECHNOLOGY, 02600, ARAU, PERLIS, MALAYSIA
[4] CZĘSTOCHOWA UNIVERSITY OF TECHNOLOGY, DEPARTMENT OF TECHNOLOGY AND AUTOMATION, 19C ARMII KRAJOWEJ AV., 42-200 CZĘSTOCHOWA, POLAND
[5] UNIVERSITI TEKNOLOGI MALAYSIA, FACULTY OF CIVIL ENGINEERING, INSTITUTE FOR SMART INFRASTRUCTURE AND INNOVATIVE CONSTRUCTION, 81310 JOHOR, MALAYSIA
[6] DEPARTMENT OF CHEMISTRY, INSTITUT TEKNOLOGI SEPULUH NOPEMBER, SURABAYA 60115, INDONESIA

* Corresponding author: wanmastura@unimap.edu.my

metal contaminant and wastewater composition, further optimizing removal efficiency.

Recently, geopolymers or alkali-activated materials (AAM) have gained acknowledgment as promising agents for treating heavy metal wastewater in industries owing to their distinct and diverse physicochemical attributes [24-26], which belong to the category of inorganic substances, primarily amorphous compounds characterized by intricate three-dimensional network structures encompassing negatively charged [AlO_4] tetrahedra and neutral [SiO_4] tetrahedra. These structures incorporate Na^{2+} or K^+ ions within a tetrahedral framework, allowing external ion exchange [27,28]. They can effectively treat heavy metal cations in wastewater by combining charge neutralization, immobilization, and adsorption [29-33].

Numerous studies have focused on the potential of geopolymer-based adsorbents for copper (Cu) removal. Baykara et al. [34] fabricated a geopolymer adsorbent using Ecuadorian zeolite-rich tuff and achieved a Cu^{2+} saturated adsorption capacity of 52.63 mg/g for Cu^{2+}. Demir et al. [35] formulated a geopolymer from gold ore waste, achieving a 99% copper-ion removal rate under specific experimental conditions. Darmayanti et al. [36] utilized alkali activated fly ash-based geopolymer resulting in a Cu^{2+} removal rate of 98 % under particular adsorption conditions.

In addition to wastewater treatment, clay minerals are widely available in nature, making them sustainable and easily accessible raw materials for AAM adsorbent supplies for large-scale applications [33,37]. By repurposing clay minerals, producing AAMs helps minimize environmental impacts and promotes circular economic principles. The calcination of clay minerals to produce metakaolin enhances its reactivity and surface properties [38-40]. This increased reactivity allows for improved binding and adsorption capabilities, making metakaolin-based AAM highly effective in applications such as heavy metal adsorption [41-43].

This study provides a comprehensive understanding of the factors influencing the Cu^{2+} adsorption process, including the initial pH and concentration of the adsorption process of Cu^{2+} through static adsorption tests. The adsorption mechanism of Cu^{2+} was also investigated by analyzing the adsorption isotherms of metakaolin-based alkali-activated materials.

2. Experimental method

2.1. Materials

To obtain reactive metakaolin (MK), the AAM precursors were sourced from Kaolin (Malaysia) Sdn. Bhd. in Bidor, Perak, Malaysia was subjected to calcination. Calcination was conducted at 850°C for 2 h at a heating rate of 5°C/min to ensure the desired transformation of the precursor into metakaolin. The elemental composition of the resulting MK is listed in TABLE 1. The analysis revealed that the primary components of the MK were alumina and silica, constituting a major portion. Minor constituents such as Na, Mg, Fe and K were also detected significantly within the metakaolin sample.

TABLE 1

Chemical Composition of Metakaolin

Raw materials (wt.%)	Si	Al	K	Fe	Na	Mg	Ti	Ca
Metakaolin	56.84	35.60	1.04	1.31	2.40	1.79	0.78	0.24

The alkali activator was sodium silicate, Na_2SiO_3 (molar ratio of SiO_2/Na_2O = 3.20) and 10M sodium hydroxide, and a NaOH solution made from analytical grade sodium hydroxide (NaOH, purity 99%). Sodium hydroxide and sodium silicate were mixed at a 0.5 Na_2SiO_3/NaOH ratio. The alkali activator was maintained at room temperature for 24 h before use to facilitate alkali activation of the precursors.

Hydrogen peroxide (H_2O_2) solution was used as the foaming agent. According to the experimental plan, 3 wt.% hydrogen peroxide was diluted to the appropriate concentrations from 30 wt.% H_2O_2 (Sigma Aldrich, Malaysia). It is significant to notice that H_2O_2 is thermodynamically unstable and quickly decomposes into water and oxygen gas, as shown by Eqs. (1) and (2), respectively. Therefore, Tween 80 or polysorbate 80 from Sigma Aldrich, Malaysia, with a composition of 70% oleic acid (primarily linoleic, palmitic, and stearic acids), was used as the foam stabilizer to reduce the surface tension and drainage of alkali-activated materials.

$$H_2O_2 + OH^- \rightarrow HO_2^- + H_2O \quad (1)$$

$$HO_2^- + H_2O_2 \rightarrow H_2O + O_2 + OH^- \quad (2)$$

2.2. Alkali Activated Materials Adsorbent Synthesis

Fig. 1 shows an illustration of the synthesis approaches for MK-based alkali-activated materials adsorbent. An alkaline activator solution made of sodium hydroxide (NaOH) and sodium silicate (Na_2SiO_3) was combined with metakaolin powder at a solid-to-liquid ratio of 0.8, which was chosen based on previous research [33,44]. The solution formed was mixed with 1.00 wt.% hydrogen peroxide and 3 wt.% Tween 80 as a foaming agent by mass of metakaolin. Consequently, the mixture was mixed to form homogenous alkali-activated materials paste. Subsequently, the resulting AAM paste was shaped into the desired shape of approximately 1 cm (forming a small round shape). The samples were placed in a steel tray and an oven for curing at 60°C for 24 h. After that, the samples were removed from the oven and crushed gently using a mortar and pestle. The following steps were repeated to prepare alkali-activated materials without a foaming agent for comparison. Then, it was sieved using a lab sieve to obtain a 150 μm particle size for further use in the adsorption test. Sieved AAM powder samples (with and without a foaming agent) were used for the adsorption test and characterization.

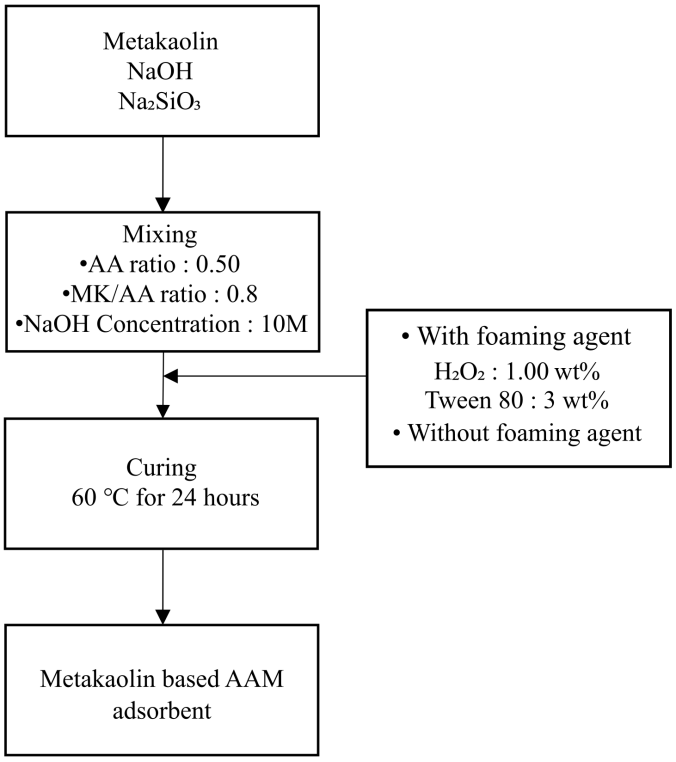

Fig. 1. Synthesis of metakaolin based alkali activated materials

2.3. Preparation of Copper Solution

Cu(II) solutions were prepared following Eq. 3 by diluting 3.929 g of analytical grade $Cu(NO_3)_2 \cdot 3H_2O$ copper stock into 1 Liter of distilled water to produce a stock solution concentration of 1000 ppm.

$$\text{Amount of metal stock, } g = = \frac{\text{Molecular weight of } Cu(NO)3.3H_2O}{\text{Atomic weight of metal ion}} \quad (3)$$

To produce a 50 ppm whereas (50 ppm = 50 mg/L) of copper nitrate solution, 50 ml of 1000 ppm copper nitrate solution was poured into the measuring cylinder and filled into the volumetric flask. Distilled water was added to the volumetric flask until it reached its upper line, producing a 50 ppm copper nitrate solution. The same was done to prepare 100, 150, 200, and 250 ppm by varying the volume added to the measuring cylinder based on the concentration to be prepared (50, 100, 150, 200, and 250 ml). Before adding the AAM adsorbent to the Cu(II) ion solutions, the pH levels were adjusted with 0.1 M NaOH and/or 0.1 M HNO_3. The pH was varied between 2,3,4,5, and 6. A digital pH meter (Hanna Instruments, HI-98107) was used to measure the pH, which was calibrated before each use.

2.4. Characterization

The chemical composition of the raw material was analyzed using a PANalytical PW4030 X-ray fluorescence (XRF) spectrometer. A TESCAN VEGA's 4th generation Scanning Electron Microscope (SEM) was used to obtain SEM micrographs and EDX spectra of metakaolin-based AAM adsorbents before and after Cu(II) adsorption. The adsorbent samples were coated with gold for 20 s to prevent electron charging during the SEM examination. The surface area, pore size distribution, and adsorption/desorption isotherm of metakaolin based AAM adsorbent were analyzed by Brunauer-Emmett-Teller (BET) Surface Area and and Barrett, Joyner, and Halenda (BJH) methods using a Micrometrics Tristar II 3020 Analyzer. X-Ray Diffraction (XRD) patterns were obtained using an XRD-6000 Shimadzu X-Ray Diffractometer with Cu Kα radiation at 30 mA and 40 kV. The XRD data was collected at 2θ values in the range from 10° to 80°.

2.5. Cu(II) Adsorption Test

Copper ions, Cu(II) adsorption experiments were conducted by mixing a measured amount of adsorbent (0.15 g) with a Cu(II) solution (100 mL) in a glass flask on a thermostatic shaker. The utilization potential of the MK-based AAM adsorbent was determined using batch adsorption tests, in which the removal efficiency of the adsorbent was studied under laboratory conditions with varying pH (2, 3, 4, 5, and 6) and initial concentrations (50, 100, 150, 200, and 250 ppm). After 1 h of contact, the mixture was centrifuged to separate the metakaolin-based AAM adsorbent from the liquid phase. The amount of Cu(II) remaining in the supernatant was measured using atomic absorption spectrometry (AAS). The adsorption capacity (q_e) in mg/g can be determined by Eq. 3 for measuring the amount of contaminant adsorbed per unit mass of the adsorbent whereas the percentage removal efficiency (%) is calculated using Eq. 4 to assess how well the MK-based alkali-activated material adsorbents performs in removing copper contaminants from the solution.

$$\text{Adsorption capacity, } q_e = \frac{(C_0 - C_e)V}{W} \quad (3)$$

$$\text{Removal efficiency, } \% = \frac{C_0 - C_e}{C_0} \times 100 \quad (4)$$

Where:

C_0 – Initial concentration of the copper solution (mg/L),
C_e – Final concentration of the copper solution after adsorption (mg/L),
W – The weight of the adsorbent usage (g),
V – The volume of the Cu(II) solution (L).

3. Results and discussion

3.1. Scanning Electron Microscopy (SEM) Analysis

The Scanning Electron Microscopy (SEM) images in Fig. 2 provide insightful differences in the microstructures of

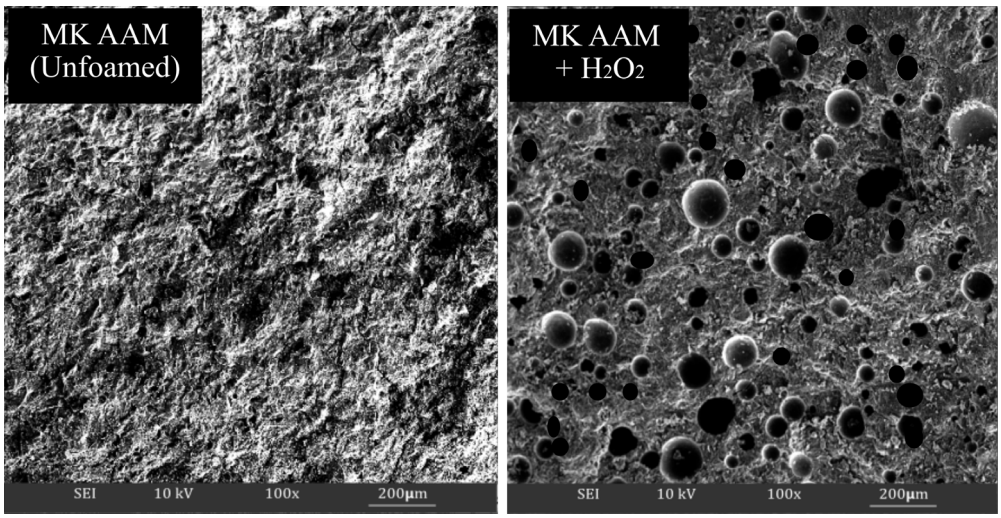

Fig. 2. Microstructure of unfoamed and foamed metakaolin based AAM

MK-based alkali-activated materials when comparing samples with and without the presence of a foaming agent (hydrogen peroxide). A dense and compact microstructure was observed in SEM images of metakaolin-based alkali-activated materials without hydrogen peroxide, H_2O_2. The matrix appeared relatively homogenous, with fewer voids or tiny pores. The absence of H_2O_2 reduces porosity and limited interconnected pathways for gas or fluid penetration [45]. This led to a more uniform surface texture with fewer irregularities. Conversely, SEM images of MK-based alkali-activated materials containing H_2O_2 exhibited a markedly different microstructure. The foaming agent contributes to forming cellular or porous structures within the material. This structure consisted of numerous interconnected voids or pores of varying sizes. The presence of the foaming agent facilitates the expansion of the material during its setting or curing process, generating a three-dimensional network of voids that significantly enhances the porosity of the material.

3.2. Brunauer-Emmett Teller (BET) Analysis

Brunauer-Emmett Teller (BET) analysis of metakaolin-based alkali-activated materials (AAM) with and without a foaming agent in TABLE 2 summarised the textural characteristics and porosity of the materials. The surface area values indicated a significant enhancement in unfoamed and foamed AAM compared to raw metakaolin. This trend is expected, as the activation process typically involves reactions that generate additional surface area owing to the formation of new phases and a more open structure [46,47]. The surface area of the unfoamed AAM (10.8483 m^2/g) was notably higher than that of raw metakaolin (4.5752 m^2/g), suggesting successful alkali activation significantly increased the surface area of alkali activated materials. However, foamed AAM exhibited an even larger surface area (28.6057 m^2/g), surpassing the unfoamed variant. Furthermore, the average pore size of the unfoamed AAM was slightly larger than that of raw metakaolin, indicating that the activation process led to the development of larger pores. This increase in the surface area is attributed to the incorporation of the foaming agent, which promotes the creation of higher porosity with larger pores and voids in the structure of the material during its setting or curing process [48-50].

3.3. X-Ray Diffraction (XRD) Analysis

Fig. 3 shows the X-ray Diffraction (XRD) diffractogram analysis of metakaolin and MK-based AAM samples. The XRD pattern of metakaolin displayed a broad peak between 15° and 30° of 2θ, typically attributed to the amorphous nature of metakaolin. Peaks corresponding to kaolinite (K) and quartz (Q) are identified in the metakaolin sample. Upon alkali activation, the XRD pattern of metakaolin-based alkali-activated materials shifted the diffuse hump towards higher angles (20°-35° 2θ), indicating the emergence of the primary binder phase in the AAM matrix. As observed through microstructural analysis,

TABLE 2

Pore structure analysis of Metakaolin (MK), Metakaolin based AAM (MK AAM) and MK-based AAM with foaming agent (MK AAM+H_2O_2)

Sample	S_{BET} (m^2/g)	Average pore size (nm)	Pore volume (cm^3/g)		
			<2 nm	2-50 nm	>50 nm
MK	4.5752	6.9267	0.000675	0.007923	0.012366
MK AAM	10.8483	15.38298	0.002271	0.052413	0.015739
MK AAM + H_2O_2	28.6057	27.1618	0.003721	0.164045	0.026582

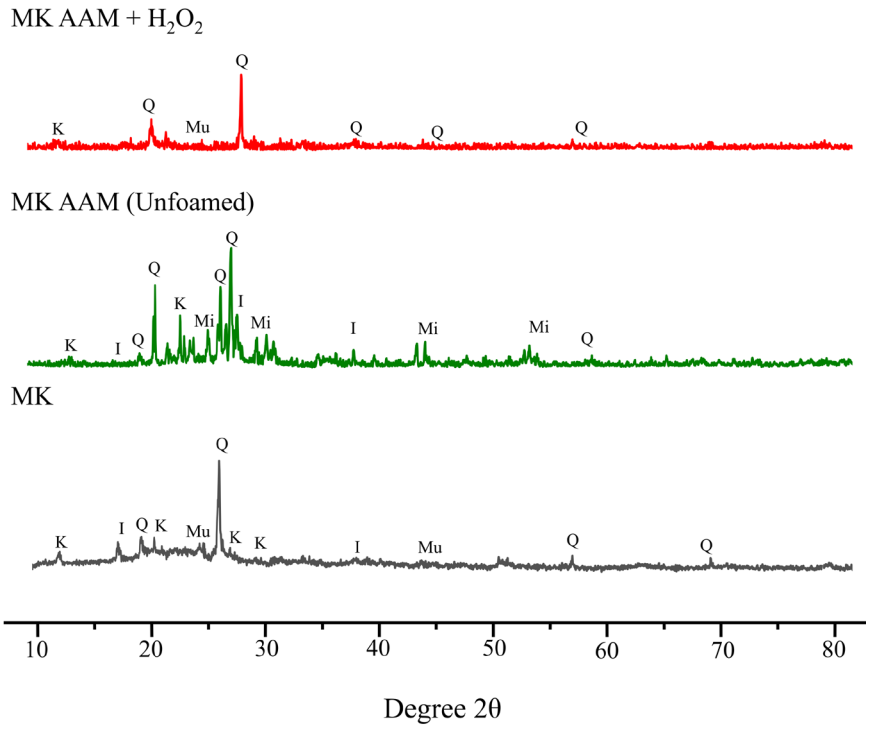

Fig. 3. XRD diffractogram of raw metakaolin, metakaolin based AAM unfoamed and metakaolin based AAM with hydrogen peroxide

the unfoamed AAM exhibited a more condensed and tightly packed arrangement, forming crystalline phases. Such compact crystalline structures typically display diminished porosity and a reduced presence of void spaces [42,51]. Moreover, identifying microline (Mi) and illite (I) in MK AAM unfoamed could indicate that the initial kaolinite mineral contained this phase, and some remnants or transformed phases might persist in the metakaolin itself.

However, the results present a fascinating scenario in which introducing hydrogen peroxide to the synthesis process of MK-based alkali-activated materials leds to an amorphous phase, possibly due to chemical reactions induced by hydrogen peroxide. Hydrogen peroxide, a strong oxidizing agent, can initiate chemical reactions that lead to the breakdown of crystalline phases into amorphous or poorly ordered structures. In addition, many kaolinite peaks disappeared because of dissolution in the alkali solution. Muscovite (Mu) minerals have cation exchange properties due to exchangeable cations in their interlayer spaces. This ion-exchange capacity allows muscovite to adsorb and release various ions, making it useful in applications where selective ion removal is desired [17,52,53]. Similarly, the quartz peak remained detectable in the MK based AAM even after the alkali activation reaction. This persistence of the quartz peak supports its insolubility and stability in the reaction environment [54,55].

3.4. Cu(II) Uptake by Metakaolin based Alkali Activated Materials

The Cu^{2+} removal efficiency of the reference MK-based AAM and porous MK-based AAM was measured under the following conditions: pH = 5, initial Cu^{2+} concentration $C_0 = 100$ ppm, contacting time $t = 90$ min and 0.15 g adsorbent at room condition. As shown in Fig. 4, the removal efficiency of the porous MK-based AAM (with hydrogen peroxide) was 99.13%; however, it was only 32.47% for the reference MK-based AAM (without hydrogen peroxide). This result indicates that alkali-activated materials synthesized from porous metakaolin and hydrogen peroxide possess a significant number of sorption sites and offer a notable advantage in enhancing the uptake percentage of Cu^{2+} [56-58]. This advantage arises from their well-defined characteristics, including higher specific surface area, average pore size, and pore volume with a porous structure, as illustrated in Fig. 2 and TABLE 2. The transformation of metakaolin into amorphous foaming porous AAM, as shown in Fig. 3, leads

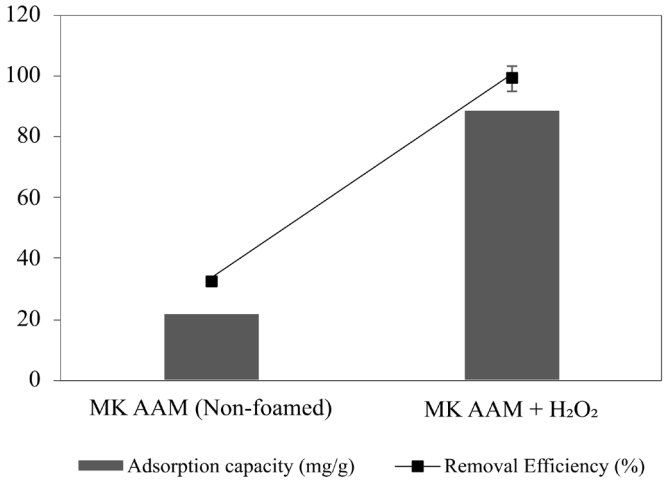

Fig. 4. Comparison between unfoamed and foamed metakaolin based AAM adsorbent on copper adsorption

to forming a porous structure that encourages Cu^{2+} sorption. This means porous metakaolin-based alkali-activated materials (AAM) have shown significant promise and advantages as adsorbents for batch adsorption experiments compared to non-foamed metakaolin-based AAM.

3.5. Adsorption Batch

Different operating parameters, such as the pH and initial concentration of the solution, were tested to study their effects on the removal of Cu(II) by the MK AAM adsorbent and to determine the adsorption properties of these materials.

3.6. Effect on Initial pH

As shown in Fig. 5, the adsorption capacity of copper (II) ions increased progressively with increasing initial pH of the solution. This trend is evident from the graph, where the adsorption capacity increased from pH 2 to 6. At pH 2, the adsorption capacity was 14.146 mg/g, which increased notably to 29.965 mg/g at pH 3. A further increase was observed at pH 4 (69.7657 mg/g), followed by significant enhancement at pH 5 (88.3720 mg/g) and pH 6 (72.6040 mg/g). The removal efficiency of Cu(II) ions also displayed an increasing trend with increasing initial pH. The percentage removal efficiency started at 21.21% at pH 2 and exhibited remarkable improvement as the pH increased. It reached 44.95% at pH 3, 89.99% at pH 4, and notably highest levels of 99.13% at pH 5. Yet, at pH 6, there was a fall to 90.75%. The optimum pH for copper ion adsorption on MK AAM is 5, which is consistent with previous research [59-61].

This trend can be attributed to the dependence of the adsorption process on pH-dependent surface charges. At lower pH values, the surface of the adsorbent material tends to carry a positive charge, which might repel the positively charged copper ions. As the pH increases (up to 5), the surface becomes less positively charged surface of the adsorbent than hydrogen ions, facilitating stronger electrostatic attraction between the adsorbent and copper ions, leading to increased adsorption capacity and removal efficiency [62,63]. However, at pH values above 5, copper hydroxide began to form, decreasing copper adsorption efficiency. This is because the surface of the adsorbent becomes more negatively charged owing to deprotonation, which results in electrostatic repulsion between the copper ions and the surface.

3.7. Effect on Initial Concentration

An inverse relationship between concentration and capacity becomes evident in the case of varying initial copper concentrations (Fig. 6). As the concentration of copper (II) ions increased, the capacity gradually decreed. This trend is visibly illustrated in the graph. Commencing at 50 ppm, the adsorption capacity was 39.3047 mg/g. As concentration rose to 100 ppm, capacity enhanced to 88.3720 mg/g. Subsequently, a gradual decline was observed at 150 ppm (72.1557 mg/g), 200 ppm (49.7867 mg/g), and 250 ppm (46.9 mg/g). The removal efficiency followed a similar decreasing trend with higher initial copper concentrations. At 50 ppm, the removal efficiency was 88.35%, then increased to 99.13% at 100 ppm. As the concentration increased, the removal efficiency dropped to 72.16% at 150 ppm, 37% at 200 ppm, and 28% at 250 ppm.

The concentration-dependent behaviour can be attributed to the limited availability of adsorption sites on the adsorbent surface. This is because the adsorbent can only bind a certain amount of copper before it becomes saturated [64,65]. The available sites are not saturated at lower concentrations (50 and 100 ppm), resulting in higher adsorption capacity and removal efficiency. However, as the concentration increases (150-250 ppm), a point is reached where the surface sites become increasingly occupied or free active surface area is reduced, leading to a decreased adsorption capacity and efficiency.

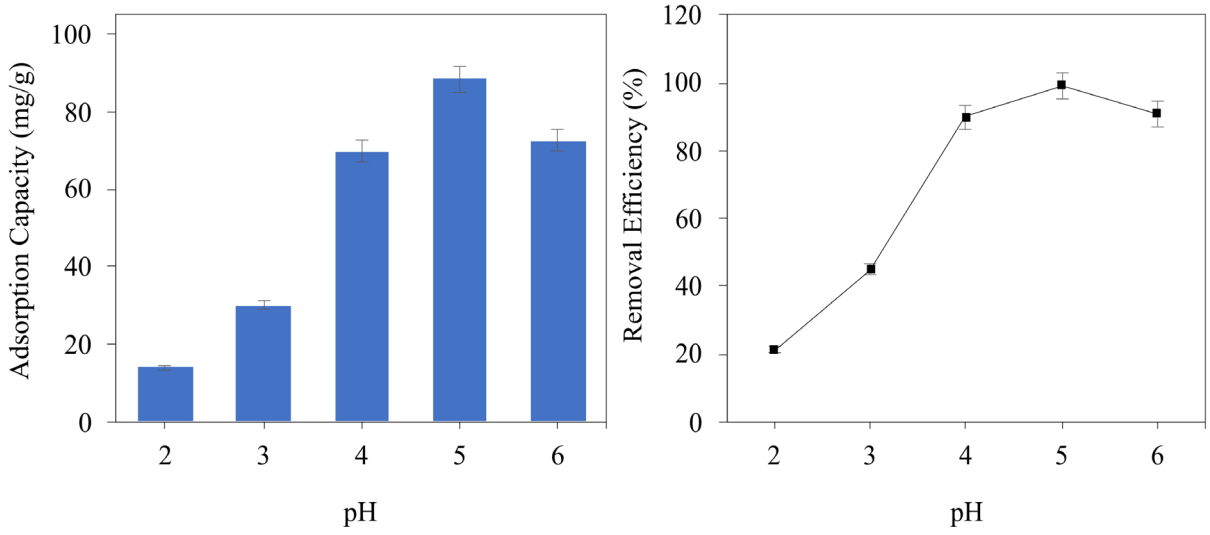

Fig. 5. Adsorption capacity and removal efficiency of the MK AAM adsorbent at different initial pH values

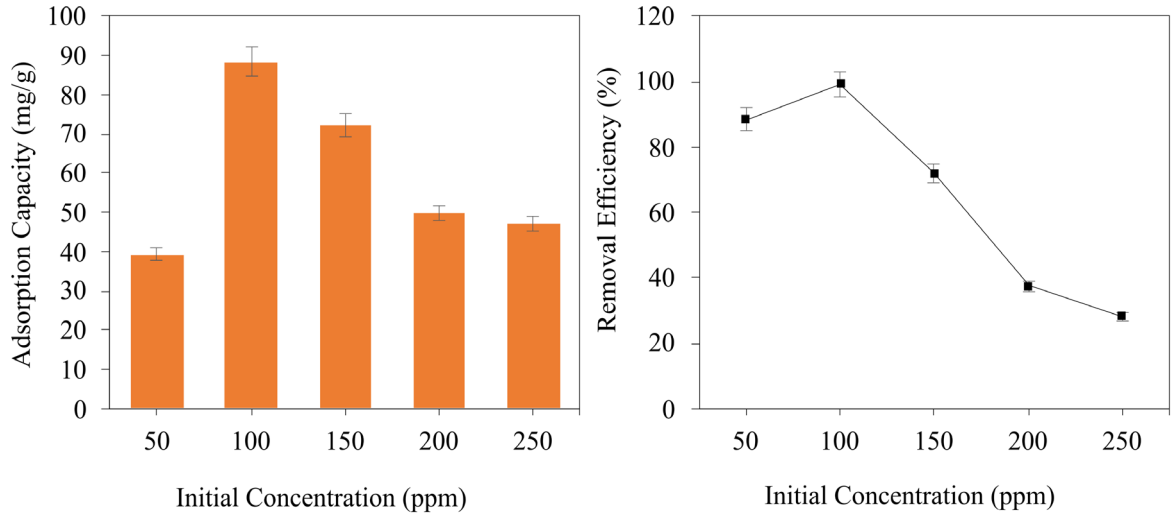

Fig. 6. Adsorption capacity and removal efficiency of MK AAM adsorbent at different initial concentration

3.8. Adsorption Isotherms

Adsorption isotherms provide valuable insights into the surface characteristics, adsorption potential, and their impact on the copper heavy metal removal process using metakaolin based alkali activated materials (MK AAM) adsorbents under different concentrations. The experiment was performed at pH 5, room temperature and 60 minutes contact time. Two widely used isotherm models, namely Langmuir and Freundlich and equations describing each isotherm are presented in TABLE 3.

TABLE 3

Isotherm adsorption models

Adsorption isotherm	Equation	Linear form
Langmuir model	$q_{eq} = \frac{q_{max} \cdot K_L \cdot C_{eq}}{1 + K_L \cdot C_{eq}}$	$\frac{1}{q_e} = \frac{1}{q_m K_L} \cdot \frac{1}{C_{eq}} + \frac{1}{q_m}$
Freundlich model	$q_{eq} = K_F \cdot C_{eq}^{1/n}$	$\ln q_e = \ln K^F + \frac{1}{n} \ln C_{eq}$

The variables q_{eq} and C_{eq} represent the adsorption capacity (mg/g) and the residual concentration of Cu(II) (mg/L) at equilibrium, respectively. The parameter q_m refers to the maximum monolayer adsorption capacity of *metakaolin* AAM adsorbent (mg/g). The Langmuir constant, K_L (L/mg), quantifies the affinity of the binding sites for the adsorbate. On the other hand, n represents the degree of dependence of adsorption on equilibrium and K_F [(mg/g)(L/mg)$^{1/n}$] are the Freundlich constants, representing the adsorption capacity and its adsorption efficiency, respectively.

A linear form of the isotherms equations was used for graphical plots of the experimental data as in Figs. 7 and 8. The models parameters were determined from the slope and the interception of the plots. Results are presented in TABLE 4.

One of the most often used equations for modeling equilibrium data in solid-liquid systems is the Langmuir isotherm

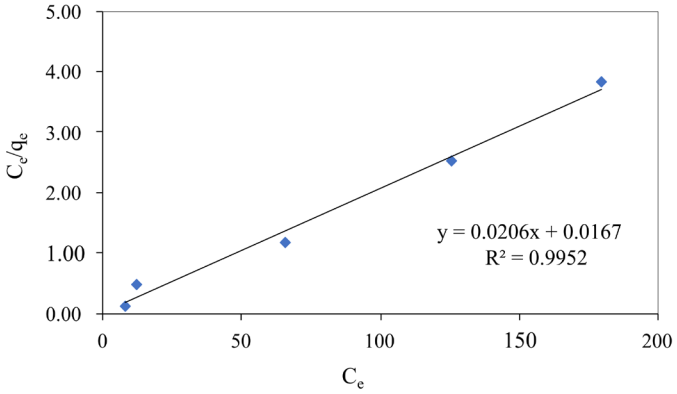

Fig. 7. Langmuir isotherm plots for Cu(II) adsorption by metakaolin based AAM

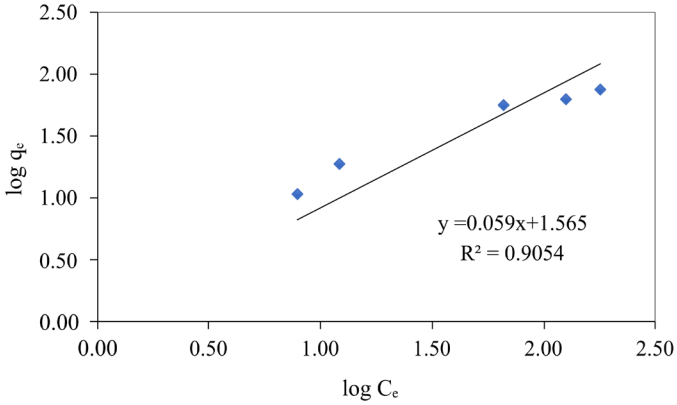

Fig. 8. Freundlich isotherm plots for adsorption of Cu(II) by metakaolin based AAM

TABLE 4

Langmuir and Freundlich parameters for Cu(II) adsorption onto metakaolin-based AAM adsorbents

pH	Langmuir isotherm			Freundlich isotherm		
	Q_{max} (mg/g)	K_L	R^2	n	K_F	R^2
5	78.544	1.2335	0.9952	16.835	36.728	0.9054

model. This formula is appropriate for monolayer adsorption onto a surface with a predetermined number of identical sites evenly distributed throughout the adsorbent surface [66-69]. The relationship between the adsorbate amount adsorbed onto the adsorbent can be explained by adsorption isotherms [70]. In this study, the magnitudes of R^2 values of Langmuir 0.9952 which was higher than Freundlich. A maximum adsorption value of 78.544 mg/g has been calculated by the Langmuir isotherm model, which is in close concurrence with the actual result of 88.372 mg/g. According to this order, it can be concluded that Cu(II) adsorption onto metakaolin based AAM was fitted using Langmuir isotherm.

4. Conclusion

This study investigates the potential of metakaolin-based alkali-activated materials (AAM) as efficient adsorbents for copper removal through adsorption. The optimization process involved comparing the synthesis of AAM using metakaolin as the precursor material under two conditions: one that added foaming agents, specifically hydrogen peroxide with a surfactant, and the other without any foaming agent. Characterization techniques, including specific surface area (BET), X-ray diffraction (XRD), and scanning electron microscopy (SEM), were employed to analyze the structural and morphological changes of the synthesized AAM. Batch adsorption experiments were conducted to evaluate the copper removal efficiency of the optimized AAM by considering factors such as initial copper concentration and pH. The results demonstrated that the optimized AAM exhibited superior copper adsorption performance, achieving a removal efficiency of over 90% under optimized conditions. The adsorption data was superior for fitting the Langmuir isotherm models, suggesting that copper ions perform as a single molecule layer for MK based AAM adsorption. This study contributes to the development of sustainable and effective materials for water treatment, particularly for addressing copper contamination. Metakaolin-based AAM with 1.00 wt.% hydrogen peroxide indicated the availability of numerous active sites for binding with Cu^{2+} and showed promise as a hight-effective, convenient, and eco-friendly adsorbent for copper removal, with potential applications in various industrial and environmental settings.

Acknowledgment

The authors would like to express the gratitude to the Japan-Asean Science, Technology & Innovation Platform (JASTIP) and the Fundamental Research Grant Scheme (FRGS) under a grant number of FRGS/1/2019/TK10/UNIMAP/02/21 from the Ministry of Higher Education Malaysia for their invaluable supports in facilitating the publication of this work.

REFERENCES

[1] T.O. Ajiboye, O.A. Oyewo, D.C. Onwudiwe, Simultaneous removal of organics and heavy metals from industrial wastewater: A review. Chemosphere **262**. Elsevier Ltd, Jan. 01 (2021). DOI: https://doi.org/10.1016/j.chemosphere.2020.128379

[2] S.O. Akinnawo, P.O. Ayadi, M.T. Oluwalope, Chemical coagulation and biological techniques for wastewater treatment. Ovidius University Annals of Chemistry **34** (1), 14-21, Jan. (2023). DOI: https://doi.org/10.2478/auoc-2023-0003

[3] Z.F. Pan, L. An, Removal of Heavy Metal from Wastewater Using Ion Exchange Membranes. In: Inamuddin, Ahamed, M., Asiri, A. (eds) Applications of Ion Exchange Materials in the Environment. Springer, Cham. (2019).
DOI: https://doi.org/10.1007/978-3-030-10430-6_2

[4] H. Peng, J. Guo, Removal of chromium from wastewater by membrane filtration, chemical precipitation, ion exchange, adsorption electrocoagulation, electrochemical reduction, electrodialysis, electrodeionization, photocatalysis and nanotechnology: a review. Environmental Chemistry Letters **18** (6), 2055-2068, Nov. 01 (2020). DOI: https://doi.org/10.1007/s10311-020-01058-x

[5] K. Saravanakumar, S. De Silva, S.S. Santosh, A. Sathiyaseelan, A. Ganeshalingam, M. Jamla, A. Sankaranarayanan, V.P. Veeraraghavan, D. MubarakAli, J. Lee, G. Thiripuranathar, Impact of industrial effluents on the environment and human health and their remediation using MOFs-based hybrid membrane filtration techniques. Chemosphere **307**, Nov. (2022).
DOI: https://doi.org/10.1016/j.chemosphere.2022.135593

[6] J. Li, J. Ma, R. Dai, X. Wang, M. Chen, T.D. Waite, Z. Wang, Self-Enhanced Decomplexation of Cu-Organic Complexes and Cu Recovery from Wastewaters Using an Electrochemical Membrane Filtration System. Environ. Sci. Technol. **55** (1), 655-664, Jan. (2021). DOI: https://doi.org/10.1021/acs.est.0c05554

[7] J. Lee, W.C. Cho, K.M. Poo, S. Choi, T.N. Kim, E.B. Son, Y.J. Choi, Y.M. Kim, Y.M. K.J. Chae, Refractory oil wastewater treatment by dissolved air flotation, electrochemical advanced oxidation process, and magnetic biochar integrated system. Journal of Water Process Engineering **36**, Aug. (2020).
DOI: https://doi.org/10.1016/j.jwpe.2020.101358

[8] G. Pooja, P.S. Kumar, G. Prasannamedha, S. Varjani, D.V.N. Vo, Sustainable approach on removal of toxic metals from electroplating industrial wastewater using dissolved air flotation. Journal of Environmental Management **295**, Oct. (2021).
DOI: https://doi.org/10.1016/j.jenvman.2021.113147

[9] C. Xu, W. Yu, K. Zheng, C. Ling, S. Yu, L. Jiang, Novel composite oxygen-containing resins with effective adsorption towards anilines: physical & chemical adsorption. Journal of Chemical Technology and Biotechnology **95** (8), 2187-2194, (2020). DOI: https://doi.org/10.1002/jctb.6405

[10] B. Nazari, S. Abdolalian, M. Taghavijeloudar, An environmentally friendly approach for industrial wastewater treatment and bio-adsorption of heavy metals using Pistacia soft shell (PSS) through flocculation-adsorption process. Environmental Research **235**, Oct. (2023).
DOI: https://doi.org/10.1016/j.envres.2023.116595

[11] S. Onutai, T. Kobayashi, P. Thavorniti, S. Jiemsirilers, The adsorption of cadmium ions on fly ash based geopolymer particles. Key Engineering Material **766**, 65-70 (2018).
DOI: https://doi.org/10.4028/www.scientific.net/KEM.766.65

[12] S.A. Rasaki, Z. Bingxue, R. Guarecuco, T. Thomas, Y. Minghui, Geopolymer for use in heavy metals adsorption, and advanced oxidative processes: A critical review. Journal of Cleaner Production **213**, 42-58 (2019).
DOI: https://doi.org/10.1016/j.jclepro.2018.12.145

[13] S.Y. Cheng, P. Show, F. Lau, J. Chang, T. C. Ling, Review New Prospects for Modified Algae in Heavy Metal Adsorption. Trends Biotechnology **37** (11), 1255-1268 (2019).
DOI: https://doi.org/10.1016/j.tibtech.2019.04.007

[14] E. Da'na, Adsorption of heavy metals on functionalized-mesoporous silica: A review. Microporous and Mesoporous Materials **247**, 145-157 (2017).
DOI: https://doi.org/10.1016/j.micromeso.2017.03.050

[15] G.T. Tee, X.Y. Gok, W.F. Yong, Adsorption of pollutants in wastewater via biosorbents, nanoparticles and magnetic biosorbents: A review. Environmental Research **212**, Sep. 01, (2022).
DOI: https://doi.org/10.1016/j.envres.2022.113248

[16] H. Jin, Y. Zhang, Q. Wang, Q. Chang, C. Li, Rapid removal of methylene blue and nickel ions and adsorption/desorption mechanism based on geopolymer adsorbent. Colloids and Interface Science Communications **45** (2021).
DOI: https://doi.org/10.1016/j.colcom.2021.100551

[17] M.A. Salam, M.R. Abukhadra, M. Mostafa, Effective decontamination of As(V), Hg(II), and U(VI) toxic ions from water using novel muscovite/zeolite aluminosilicate composite: adsorption behavior and mechanism. Environmental Science and Pollution Research **27** (12), 13247-13260 (2020).
DOI: https://doi.org/10.1007/s11356-020-07945-8

[18] K. Liang, X.Q. Wang, C.L. Chow, D. Lau, A review of geopolymer and its adsorption capacity with molecular insights: A promising adsorbent of heavy metal ions. Journal of Environmental Management **322**, Nov (2022).
DOI: https://doi.org/10.1016/j.jenvman.2022.116066

[19] B.I. El-Eswed, Solidification Versus Adsorption for Immobilization of Solidification Versus Adsorption for Immobilization of Pollutants in Geopolymeric Materials: A Review. Solidification, (2018).
DOI: https://doi.org/10.5772/intechopen.72299

[20] Q. Tang, K. Wang, J. Su, Y. Shen, S. Yang, Y. Ge, X. Cui, Facile fabrication of inorganic polymer microspheres as adsorbents for removing heavy metal ions. Material Research Bulletin **113**, 202-208 (2019).
DOI: https://doi.org/10.1016/j.materresbull.2019.02.009

[21] E.C. Emenike, A.G. Adeniyi, P.E. Omuku, K.C. Okwu, K.O. Iwuozor, Recent advances in nano-adsorbents for the sequestration of copper from water. Journal of Water Process Engineering **47**, Jun. (2022).
DOI: https://doi.org/10.1016/j.jwpe.2022.102715

[22] D.G. Della Rocca, R.M. Peralta, R.A. Peralta, E. Rodríguez-Castellón, R. de Fatima Peralta Muniz Moreira, Adding value to aluminosilicate solid wastes to produce adsorbents, catalysts and filtration membranes for water and wastewater treatment. Journal Material Scince **56** (2) 1039-1063 (2021).
DOI: https://doi.org/10.1007/s10853-020-05276-0

[23] P. Arokiasamy, M.M.A.B. Abdullah, S.Z. Abd Rahim, M.R.R.M.A. Zainol, M.A.A.M. Salleh, M. Kheimi, J. Chaiprapa, A.V. Sandu, P. Vizureanu, R.A. Razak, N.H. Jamil, Metakaolin/sludge based geopolymer adsorbent on high removal efficiency of Cu^{2+}. Case Studies in Construction Materials **17**, Dec. (2022).
DOI: https://doi.org/10.1016/j.cscm.2022.e01428

[24] A.A. Siyal, M.R. Shamsuddin, M.I. Khan, N.E. Rabat, M. Zulfiqar, Z. Man, J. Siame, K.A. Azizli, A Review on Geopolymers as Emerging Materials for the Adsorption of Heavy Metals and Dyes. Journal of Environmental Management **224**, 327-339 (2018).
DOI: https://doi.org/10.1016/j.jenvman.2018.07.046

[25] E. Papa, M. Minelli, M.C. Marchioni, E. Landi, F. Miccio, A.N. Murri, P. Benito, A. Vaccari, V. Medri, Metakaolin-based geopolymer–Zeolite NaA composites as CO_2 adsorbents. Applied Clay Science **237**, 106900, Jun. (2023).
DOI: https://doi.org/10.1016/j.clay.2023.106900

[26] M. Bilal, I. Ihsanullah, M. Younas, M.U.H. Shah, Recent advances in applications of low-cost adsorbents for the removal of heavy metals from water: A critical review. Separation and Purification Technology **278**, 119510 (2022).
DOI: https://doi.org/10.1016/j.seppur.2021.119510

[27] T. Suwan, P. Jitsangiam, H. Thongchua, U. Rattanasak, W. Tangchirapat, P. Maichin, Role of Alkaline Constituent On Properties And Microstructure of Crushed Rock Based Alkali- Activated Material For Low Strength Applications. (2021).
DOI: https://doi.org/10.21203/rs.3.rs-772525/v1

[28] T. Luukkonen, Z. Abdollahnejad, J. Yliniemi, P. Kinnunen, M. Illikainen, One-part alkali-activated materials: A review. Cement and Concrete Research **103**, 21-34 (2018).
DOI: https://doi.org/10.1016/j.cemconres.2017.10.001

[29] B.C. Mendes, L.G. Pedroti, C.M.F. Vieira, M. Marvila, A.R. Azevedo, J.M.F. De Carvalho, J.C.L. Ribeiro, Application of eco-friendly alternative activators in alkali-activated materials: A review. Journal of Building Engineering **35**, no. August 2020, (2021). DOI: https://doi.org/10.1016/j.jobe.2020.102010

[30] P. Perumal, T. Luukkonen, H. Sreenivasan, P. Kinnunen, M. Illikainen, Porous alkali-activated materials. In New Materials in Civil Engineering, 529-563 (2020).
DOI: https://doi.org/10.1016/b978-0-12-818961-0.00015-6

[31] K. Gruskevica, G. Bumanis, K. Tihomirova, D. Bajare, T. Juhna, Alkaline activated material as the adsorbent for uptake of high concentration of zinc from wastewater. Key Engineering Material **721**, 123-127 (2017).
DOI: https://doi.org/10.4028/www.scientific.net/kem.721.123

[32] T. Luukkonen, A. Heponiemi, H. Runtti, J. Pesonen, J. Yliniemi, U. Lassi, Application of alkali-activated materials for water and wastewater treatment: a review. Reviews in Environmental Science and Bio/Technology **18** (2), 271-297 (2019).
DOI: https://doi.org/10.1007/s11157-019-09494-0

[33] M. Ibrahim, W.M. Wan Ibrahim, M.M.A.B. Abdullah, M. Nabialek, R. Putra Jaya, M. Setkit, R. Ahmad, B. Jez, Synthesis of Metakaolin Based Alkali Activated Materials as an Adsorbent at

Different Na_2SiO_3/NaOH Ratios and Exposing Temperatures for Cu^{2+} Removal. Materials **16**, 3, Feb. (2023).
DOI: https://doi.org/10.3390/ma16031221

[34] H. Baykara, M.D.L.M. Solorzano, J.J.D. Echeverria, M.H. Cornejo, C.V. Tapia-Bastidas, The use of zeolite-based geopolymers as adsorbent for copper removal from aqueous media. Royal Society Open Science **9**, 3 (2022).
DOI: https://doi.org/10.1098/rsos.211644

[35] F. Demir, E. Moroydor Derun, Usage of gold mine tailings based geopolymer on Cu^{2+} adsorption from water. Main Group Chemistry **18**, 4, 467-476 (2019).
DOI: https://doi.org/10.3233/MGC-190801

[36] L. Darmayanti, S. Notodarmojo, E. Damanhuri, G.T.M. Kadja, Preparation of alkali-activated fly ash-based geopolymer and their application in the adsorption of copper (II) and zinc (II) ions. **12**, 0-11 (2019).
DOI: https://doi.org/10.1051/matecconf/201927606012

[37] K. Trivunac, L.M. Kljajevic, S. Nenadovic, Microstructural characterization and adsorption properties of alkali-activated materials based on metakaolin. Science of Sintering **48** (2), 209-220 (2016).
DOI: https://doi.org/10.2298/SOS1602209T

[38] A. Kaddami, O. Pitois, Cement and Concrete Research A physical approach towards controlling the microstructure of metakaolin-based geopolymer foams. Cement and Concrete Research **124**, no. June, (2019).
DOI: https://doi.org/10.1016/j.cemconres.2019.105807

[39] M.F. Zawrah, S.E. Abo Sawan, R.M. Khattab, A.A. Abdel-Shafi, Effect of nano sand on the properties of metakaolin-based geopolymer: Study on its low rate sintering. Construction Building Materials **246** (2020).
DOI: https://doi.org/10.1016/j.conbuildmat.2020.118486

[40] A.S. Sauffi, W.M. Wan Ibrahim, M.M. Al Bakri Abdullah, M. Ibrahim, R. Ahmad, F.A. Zaidi, Phase Analysis Of Different Liquid Ratio On Metakaolin/Dolomite Geopolymer. Archives of Metallurgy and Materials **67**, 1, 247-250 (2022).
DOI: https://doi.org/10.24425/amm.2022.137497

[41] M. Ibrahim, W.M. Wan Ibrahim, M.M. Al Bakri Abdullah, A. S.Sauffi, A Review of Geopolymer Based Metakaolin Membrane as an Effective Adsorbent for Waste Water Treatment. IOP Conference Series Materials Science Engineering **864**, 1, (2020).
DOI: https://doi.org/10.1088/1757-899X/864/1/012128

[42] T.R. Barbosa, E.L. Foletto, G.L. Dotto, S.L. Jahn, Preparation of mesoporous geopolymer using metakaolin and rice husk ash as synthesis precursors and its use as potential adsorbent to remove organic dye from aqueous solutions. Ceramic International **44**, 1, 416-423 (2018).
DOI: https://doi.org/10.1016/j.ceramint.2017.09.193

[43] P. Arokiasamy, M.M.A.B. Abdullah, S.Z. Abd Rahim, M. Sadique, L.Y. Ming, M.A.A.M. Salleh, M.R.R.M.A. Zainol, C.M.R. Ghazali, Diverse material based geopolymer towards heavy metals removal: A review. Journal of Materials Research and Technology, vol. **22**. Elsevier Editora Ltda, 126-156, Jan. 01, (2023).
DOI: https://doi.org/10.1016/j.jmrt.2022.11.100

[44] M. Ibrahim, W.M. Wan Ibrahim, M.M.A.B. Abdullah, A.S. Sauffi, P. Vizureanu, Effect of Solids-To-Liquids and Na_2SiO_3-To-NaOH on Metakaolin Membrane Geopolymers. Archieves Metallargy and Materials **67**, 695-702 (2022).
DOI: https://doi.org/10.24425/amm.2022.137808

[45] N.A. Jaya, L. Yun-Ming, H. Cheng-Yong, M.M.A.B. Abdullah, K. Hussin, Correlation between pore structure, compressive strength and thermal conductivity of porous metakaolin geopolymer. Construction Building Materials **247**, 118641 (2020).
DOI: https://doi.org/10.1016/j.conbuildmat.2020.118641

[46] A.Z. Khalifa, O. Cizer, Y. Pontikes, A. Heath, P. Patureau, S.A. Bernal, A.T. Marsh, Advances in alkali-activation of clay minerals. Cement and Concrete Research **132**. Elsevier Ltd, Jun. 01, (2020).
DOI: https://doi.org/10.1016/j.cemconres.2020.106050

[47] A.M. Elgarahy, A. Maged, M.G. Eloffy, M. Zahran, S. Kharbish, K.Z. Elwakeel, A. Bhatnagar, Geopolymers as sustainable eco-friendly materials: Classification, synthesis routes, and applications in wastewater treatment. Separation and Purification Technology **324**, 124631, Nov. (2023).
DOI: https://doi.org/10.1016/j.seppur.2023.124631

[48] D. T. Hermann, S. Tome, V.O. Shikuku, J.B. Tchuigwa, C. Janiak, M.A. Etoh, D.D. Joh Dina, Enhanced Performance of Hydrogen Peroxide Modified Pozzolan-Based Geopolymer for Abatement of Methylene Blue from Aqueous Medium. Silicon **14** (10), 5191-5206 (2022).
DOI: https://doi.org/10.1007/s12633-021-01264-4/Published

[49] Y. Hao, G. Yang, K. Liang, Development of fly ash and slag based high-strength alkali-activated foam concrete. Cememnt Concrcrete Composite **128**, Apr. (2022).
DOI: https://doi.org/10.1016/j.cemconcomp.2022.104447

[50] Y. Chen, N. Wang, O. Ola, Y. Xia, Y. Zhu, Porous ceramics: Light in weight but heavy in energy and environment technologies. Materials Science and Engineering R: Reports **143**. Elsevier Ltd, Jan. 01, (2021).
DOI: https://doi.org/10.1016/j.mser.2020.100589

[51] Q. Tang, K. Wang, M. Yaseen, Z. Tong, X. Cui, Synthesis of highly efficient porous inorganic polymer microspheres for the adsorptive removal of Pb^{2+} from wastewater. Journal of Cleaner Production **193**, 351-362 (2018).
DOI: https://doi.org/10.1016/j.jclepro.2018.05.094

[52] H. Wu, S. Lin, X. Cheng, J. Chen, Y. Ji, D. Xu, M. Kang, Comparative study of strontium adsorption on muscovite, biotite and phlogopite. Journal of Environment Radioactivity **225**, no. September, p. 106446 (2020).
DOI: https://doi.org/10.1016/j.jenvrad.2020.106446

[53] W. Zhou, J. Niu, W. Xiao, L. Ou, Adsorption of bulk nanobubbles on the chemically surface-modified muscovite minerals. Ultrasonics Sonochemistry **51**, no October 2018, pp. 31–39 (2019).
DOI: https://doi.org/10.1016/j.ultsonch.2018.10.021

[54] B. Aouan, S. Alehyen, M. Fadil, M.E. Alouani, A. Khabbazi, A. Atbir, M.H. Taibi, Compressive strength optimization of metakaolin-based geopolymer by central composite design. Chemical Data Collections **31**, 100636 (2021).
DOI: https://doi.org/10.1016/j.cdc.2020.100636

[55] M. El Alouani, S. Alehyen, M. El Achouri, M. Taibi, Preparation, Characterization, and Application of Metakaolin-Based Geopoly-

mer for Removal of Methylene Blue from Aqueous Solution. Journal of Chemistry **2019** (1), 4212901 (2019).
DOI: https://doi.org/10.1155/2019/4212901

[56] A. Maleki, Z. Hajizadeh, V. Sharifi, Z. Emdadi, A green, porous and eco-friendly magnetic geopolymer adsorbent for heavy metals removal from aqueous solutions. Journal of Cleaner Production **215**, 1233-1245, Apr. (2019).
DOI: https://doi.org/10.1016/j.jclepro.2019.01.084

[57] S. Onutai, T. Kobayashi, P. Thavorniti, S. Jiemsirilers, Porous fly ash-based geopolymer composite fiber as an adsorbent for removal of heavy metal ions from wastewater. Materials Letter **236**, 30-33 (2019).
DOI: https://doi.org/10.1016/j.matlet.2018.10.035

[58] N. Ariffin, M.M.A.B. Abdullah, P. Postawa, S.Z. Abd Rahim, M.R.R. Mohd Arif Zainol, R. Putra Jaya, A. Sliwa, M.F. Omar, J.J. Wysłocki, K. Błoch, M. Nabiałek, Effect of aluminium powder on kaolin-based geopolymer characteristic and removal of Cu^{2+}. Materials **14**, 4, 1-19 (2021).
DOI: https://doi.org/10.3390/ma14040814

[59] S. Tunali Akar, H. Colo, F. Sayin, I. Kara, T. Akar, Parametric optimization of Cu(II) removal process by a metakaolin-based geopolymer: Batch and continuous process design. Journal of Cleaner Production **366**, Sep. (2022).
DOI: https://doi.org/10.1016/j.jclepro.2022.132819

[60] Z. Yu, W. Song, J. Li, Q. Li, Improved simultaneous adsorption of Cu(II) and Cr(VI) of organic modified metakaolin-based geopolymer. Arabian Journal of Chemistry **13**, 3, 4811-4823, Mar. (2020).
DOI: https://doi.org/10.1016/j.arabjc.2020.01.001

[61] W.S. Chen, Y.C. Chen, C.H. Lee, Modified Activated Carbon for Copper Ion Removal from Aqueous Solution. Processes **10**, 1, Jan. (2022).
DOI: https://doi.org/10.3390/pr10010150

[62] M.R. Awual, Novel ligand functionalized composite material for efficient copper(II) capturing from wastewater sample. Composites Part B: Engineering **172**, 387-396, Sep. (2019).
DOI: https://doi.org/10.1016/j.compositesb.2019.05.103

[63] K.T. Kubra, M.S. Salman, M.N. Hasan, A. Islam, M.M. Hasan, M.R. Awual, Utilizing an alternative composite material for effective copper(II) ion capturing from wastewater. Journal of Molecular Liquids **336**, Aug. (2021).
DOI: https://doi.org/10.1016/j.molliq.2021.116325

[64] Q. Su, Q. Ye, L. Deng, Y. He, X. Cui, Prepared self-growth supported copper catalyst by recovering Cu (II) from wastewater using geopolymer microspheres. Journal of Cleaner Production **272**, 122571 (2020).
DOI: https://doi.org/10.1016/j.jclepro.2020.122571

[65] S. Mingming, Z. Hengze, L. Ye, Z. Lingqi, The adsorption properties of steel slag-based porous geopolymer for Cu^{2+} removal. Mineral Engineering **201**, Oct. (2023).
DOI: https://doi.org/10.1016/j.mineng.2023.108225

[66] J. Karuppaiyan, A. Mullaimalar, R. Jeyalakshmi, Adsorption of dyestuff by nano copper oxide coated alkali metakaoline geopolymer in monolith and powder forms: Kinetics, isotherms and microstructural analysis. Environmental Research **218**, Feb. (2023). DOI: https://doi.org/10.1016/j.envres.2022.115002

[67] S. Yan, F. Zhang, L. Wang, Y. Rong, P. He, D. Jia, J. Yang, A green and low-cost hollow gangue microsphere/geopolymer adsorbent for the effective removal of heavy metals from wastewaters. Journal of Environmental Management **246**, 174-183, Sep. (2019).
DOI: https://doi.org/10.1016/j.jenvman.2019.05.120

[68] T.H. Tan, K.H. Mo, S.H. Lai, T.C. Ling, Synthesis of porous geopolymer sphere for Ni(II) removal. Ceramic International **47**, 20, 29055-29063, Oct. (2021).
DOI: https://doi.org/10.1016/j.ceramint.2021.06.268

[69] A.A. Siyal, M.R. Shamsuddin, N.E. Rabat, M. Zulfiqar, Z. Man, A. Low, Fly ash based geopolymer for the adsorption of anionic surfactant from aqueous solution. Journal of Cleaner Production **229**, 232-243, Aug. (2019).
DOI: https://doi.org/10.1016/j.jclepro.2019.04.384

[70] I. Kara, D. Yilmazer, S.T. Akar, Metakaolin based geopolymer as an effective adsorbent for adsorption of zinc(II) and nickel(II) ions from aqueous solutions. Applied Clay Science **139**, 54-63 (2017). DOI: https://doi.org/10.1016/j.clay.2017.01.008